UNIVERSITY OF WEST BOHEMIA

Applied and Computational Mechanics 1 (2007) 343 - 350

Applied and Computational Mechanics

Aerodynamically generated noise by lightning arrester

J. Váchová [a,*]

[a] *ŠKODA VÝZKUM s.r.o., Tylova 1/57, 316 00 Plzeň, Czech Republic*

Received 7 September 2007; received in revised form 27 September 2007

Abstract

This paper presents the general solution of aerodynamically generated noise by lightning arrester. Governing equations are presented in form of Lighthill acoustic analogy, as embodied in the Ffowcs Williams-Hawkings (FW-H) equation. This equation is based on conservation laws of fluid mechanics rather than on the wave equation. Thus, the FW-H equation is valid even if the integration surface is in nonlinear region. That's why the FW-H method is superior in aeroacoustics. The FW-H method is implemented in program Fluent and the numerical solution is acquired by Fluent code.

The general solution of acoustic signal generated by lightning arrester is shown and the results in form of acoustic pressure and frequency spectrum are presented. The verification of accuracy was made by evaluation of Strouhal number. A comparison of Strouhal number for circumfluence of a cylinder and the lightning arrester was done, because the experimental data for cylinder case are known and these solids are supposed to be respectively in shape relation.

Keywords: aeroacoustics, acoustics, FW-H, Lighthill, Strouhal number, lightning arrester

1. Introduction

In recent years, as engineering design of components and systems has become increasingly sophisticated, a significant amount of effort has been directed toward the reduction of aerodynamically generated noise. With the ongoing advances in computational resources and algorithms, CFD (Computational Fluid Dynamics) is being used more and more to study acoustic phenomena. Through detailed simulations of fluid flow, CFD has become a viable means of gaining insight into noise sources and basic sound production mechanisms. Sound transmission from a point source to a receiver can be computed by an analytical formulation.

2. The Governing Equations

The Lighthill acoustic analogy [5], [6] provides a mathematical foundation for integral approach. The Ffowcs-Williams and Hawkings (FW-H) method [4] extends the analogy to cases where solid, permeable, or rotating surfaces are sound sources, and represents the most complete formulation of the acoustic analogy to date. The FW-H method is implemented in Fluent, described in [9].

2.1. Lighthill Acoustic Analogy

From [5], the propagation of sound in a uniform medium without sources of matter or

* Corresponding author. Tel.: +420 732 062 209, e-mail: jana.vachova@skodavyzkum.cz.

external forces is governed by mass conservation and Navier-Stokes momentum equations.

$$\frac{\partial \rho}{\partial t} - \frac{\partial}{\partial x_i} \rho u_i = 0 \tag{1}$$

$$\frac{\partial}{\partial t}(\rho u_i) + \frac{\partial}{\partial x_j}\left(\rho u_i u_j + P_{ij}\right) = 0 \tag{2}$$

where ρ is density, u_i, u_j are the velocity components and P_{ij} is the stress tensor

$$P_{ij} = p_0 \delta_{ij} - \mu \left[\frac{\partial u_i}{\partial x_j} + \frac{\partial u_j}{\partial x_i} - \frac{2}{3} \frac{\partial u_k}{\partial x_k} \delta_{ij} \right],$$

where p_0 is the static pressure of the flow field, μ is the coefficient of viscosity and δ_{ij} is the Kronecker delta. Taking the time derivative of equation (1), subtracting the divergence of equation (2), and then rearranging terms, the equation of sound propagation will be

$$\frac{\partial^2 \rho}{\partial t^2} - a_0^2 \nabla^2 \rho = \frac{\partial^2}{\partial x_i \partial x_j} T_{ij}, \tag{3}$$

where a_0 is speed of sound in a medium at rest and T_{ij} is Lighthill stress tensor defined as

$$T_{ij} = \rho u_i u_j + P_{ij} - a_0^2 \rho \delta_{ij}. \tag{4}$$

Mathematically, equation (3) is a hyperbolic partial differential equation, which describes a wave propagating at speed of sound in a medium at rest, on which fluctuating forces are externally applied in the form described by the right hand side of equation (3).

2.2. Ffowcs-William and Hawkings Method

FW-H equation is the most general form of Lighthill acoustic analogy derived by J. E. Ffowcs-Williams a D. L. Hawkings in [4] and is appropriate for predicting the noise generated from turbulence, jet noise, cavity noise, rotating surface noise.

In [1], the FW-H equation can be derived by embedding the exterior problem in unbounded space by using generalized functions to describe the flowfield. Consider a moving surface $f(x,t)=0$ with stationary fluid outside. The surface $f=0$ is defined such that $\nabla f = \hat{\boldsymbol{n}}$, where $\hat{\boldsymbol{n}}$ is a unit normal vector that points into the fluid. Inside $f=0$, the generalized flow variables are defined as having their freestream values; that is,

the density: $$\tilde{\rho} = \begin{cases} \rho & f > 0 \\ \rho_0 & f < 0 \end{cases}, \tag{5}$$

the momentum: $$\tilde{\rho}\tilde{u}_i = \begin{cases} \rho u_i & f > 0 \\ 0 & f < 0 \end{cases}, \tag{6}$$

the compressive stress tensor: $$\tilde{P}_{ij} = \begin{cases} P_{ij} & f > 0 \\ 0 & f < 0 \end{cases}. \tag{7}$$

Note that it was absorbed the constant $p_0\delta_{ij}$ into the definition of P_{ij} for convenience. Hence, for inviscid fluid, $P_{ij} = p'\delta_{ij}$, where p' is the acoustic pressure ($p' = p - p_0$). Freestream quantities are indicated by subscript 0. The summation convention is used when vector or tensor components have indices i and j.

By using definitions of equations (5), (6), (7), a generalized continuity equation can be written as

$$\frac{\bar{\partial}\tilde{\rho}}{\partial t} + \frac{\bar{\partial}\tilde{\rho}\tilde{u}_i}{\partial x_i} = \left(\rho' \frac{\partial f}{\partial t} + \rho u_i \frac{\partial f}{\partial x_i}\right)\delta(f), \tag{8}$$

where the bar in $\frac{\bar{\partial}}{\partial t}$, $\frac{\bar{\partial}}{\partial x_i}$ indicates that generalized differentiation is implied, the density $\rho' \equiv \rho - \rho_0$ and $\delta(f)$ is the one-dimensional delta function, which is zero everywhere except where f=0. The surface f=0 is often assumed to be both coincident with the body and impenetrable, but clearly choosing the integration surface coincident with the physical body is not necessary, as presented in [2], [3]. The generalized continuity equation is valid for the entire space, both inside and outside the body surface. The generalized momentum equation can be written as

$$\frac{\bar{\partial}\tilde{\rho}\tilde{u}_i}{\partial t} + \frac{\bar{\partial}\tilde{\rho}\tilde{u}_i\tilde{u}_j}{\partial x_j} + \frac{\bar{\partial}\tilde{P}_{ij}}{\partial x_j} = \left(\rho u_i \frac{\partial f}{\partial t} + (\rho u_i u_j + P_{ij})\frac{\partial f}{\partial x_j}\right)\delta(f) \tag{9}$$

Now eliminate the momentum $\tilde{\rho}\tilde{u}_i$ from both generalized equations (8), (9) by the same arrangement as in previous section, by arrangements coupled with Lighthill stress tensor (4) and with expressions $\partial f / \partial t = -v_n$, $\partial f / \partial x_i = \hat{n}_i$ and $u_n = u_i \hat{n}_i$, which is fluid velocity in the direction normal to the surface f=0. The left hand side of FW-H equation can be written as

$$\frac{\partial^2 \rho'}{\partial t^2} - \frac{\partial^2}{\partial x_i \partial x_j} a_0^2 \rho' \delta_{ij} = \frac{1}{a_0^2}\frac{\partial^2 p'(x,t)}{\partial t^2} - \nabla^2 p'(x,t) = \Box^2 \; p'(x,t), \tag{10}$$

where the customary notation $p' = c^2 \rho'$ was used, because the observer location is outside the source region. Operator $\Box^2$ is so called wave operator, which is $(1/a_0^2)(\partial^2/\partial t^2) - \nabla^2$.

The FW-H equation can be written as

$$\Box^2 p'(x,t) = \underbrace{\frac{\partial^2}{\partial x_i \partial x_j}\{T_{ij} H(f)\}}_{Quadrupole\ source} - \underbrace{\frac{\partial}{\partial x_i}\{[P_{ij}\hat{n}_j + \rho u_i (u_n - v_n)]\delta(f)\}}_{Dipol\ source} + \underbrace{\frac{\partial}{\partial t}\{[\rho_o v_n + \rho(u_n - v_n)]\delta(f)\}}_{Monopol\ source} \tag{11}$$

where v_n is the surface velocity in the direction normal to the surface $f(x,t)$=0 and $H(f)$ is Heaviside function (0 for f<0, 1 for f>0). Generally, acoustic pressure p' which is mentioned in equations (10), (11) is composed as

$$p'(\mathbf{x},t) = p'_T(\mathbf{x},t) + p'_L(\mathbf{x},t) + p'_Q(\mathbf{x},t),$$

where $p'_T(\mathbf{x},t)$ is acoustic pressure caused by monopole source (thickness noise) determined completely by the geometry and kinematics of the body. Acoustic pressure $p'_L(\mathbf{x},t)$ is caused by a dipole source (known as loading noise) generated by the force acting on the fluid as a result of the presence of the body. The classification of thickness and loading noise is related to the thickness and loading problems of linearized aerodynamics. Thus, this terminology is consistent with that of aerodynamics. Acoustic pressure $p'_Q(\mathbf{x},t)$ is caused by quadrupole source. Quadrupole source term accounts for nonlinear effects, e.g., nonlinear wave propagation and steeping, variations in local sound speed, and noise generated by shocks, vorticity, and turbulence in the flowfield.

Acoustic analogy essentially decouples the propagation of sound from its generation, allowing one to separate the flow solution process from the acoustic analysis. Hence the problem is divided into two phases. Let's call it inner problem and outer problem.

When the inner problem is solved, the transient numerical solution is realized with use of Navier-Stokes equations and very small time step (10^{-5} s). During this numerical simulation the relevant source data (pressure, velocity, density) at all face elements of the selected source surface f=0 is written on the specific files.

The outer problem is based on the Huygens-Fresnel principle, which says that each point of an advancing wave front is in fact the center of a fresh disturbance and the source of a new train of waves; and that the advancing wave as a whole may be regarded as the sum of all the secondary waves arising from points in the medium already traversed. So the analytical solution is realized when wave equation is solved from the source data. Hence the acoustic pressure is acquired in arbitrary position of acoustic field. The time dependence of acoustic pressure is transformed by Fast Fourier Transformation (FFT) to a harmonic expression of signal, which is frequency spectrum. The scheme of the solution is in figure 1.

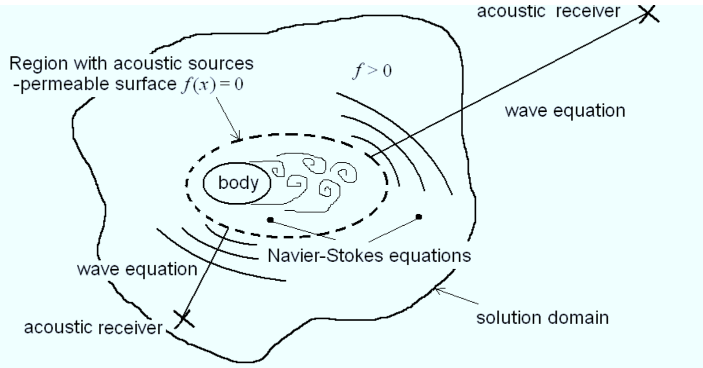

Fig. 1. The scheme of acoustic analogy approach by FW-H method.

3. Numerical Solution of the Aerodynamically Generated Noise by Lightning Arrester

The Lightning Arrester is positioned on the roof of electric locomotive. Supposed locomotive speed is 200 km/h (56 m/s). The aim of this paper was to find out the acoustic field characteristics in given positions of receivers by the FW-H method that is implemented in Fluent.

3.1. Pre-processing

By preprocessor Gambit 2.3.16, where the model and its mesh is modeled, the mathematical surface $f(x,t)$=0 around lightning arrester was prepared to include the contributions from all sources: monopole, dipole and quadrupole, see fig. 1. Thus the mathematical surface $f(x,t)$=0 is called *source surface*. There is non-moving body in the case of circumfluence, which implies that the mathematical form of source surface isn't time dependent, thus $f(x)$=0 and v_n from equation (11) is zero. In equation (11), there is used the mathematical surface identical with the body surface. But in case of lightning arrester the mathematical surface had to be modeled around the body to include quadrupole source, since as it is presented in [9] the quadrupole sources are accounted only inside the source surface. So if the conditions of Heaviside function as presented in (11) govern the quadrupole noise isn't accounted. Thus the conditions of Heaviside function is changed to $H(f)=1$ for $f<0$ and then in the FW-H method slightly different mathematical manipulations are used, as presented in [2], [3].

In preprocessing the unstructured mesh volumes were created by hex elements. The number of elements is more then 6 million. Inside the source surface $f(x)=0$, the fine mesh was used to ensure the sinusoidal acoustic signal, which corresponds to the smallest wave length of audible frequency (20000 Hz).

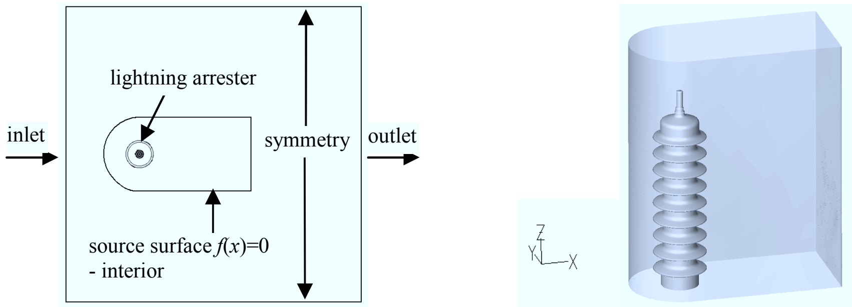

Fig. 2. Solution domain and source surface created around the lightning arrester.

The mathematical surface $f(x)$ =0 is permeable due to *interior* boundary condition, fig. 2. Side walls of solution domain are in sufficient distance from the lightning arrester and they were signified as *symmetry*.

3.2. Inner Problem Solution

After reasonably converged stationary solution, the LES (Large Eddy Simulation) approach to turbulence modeling is activated, and the source data are written to the source files, which corresponds to the source surface's elements.

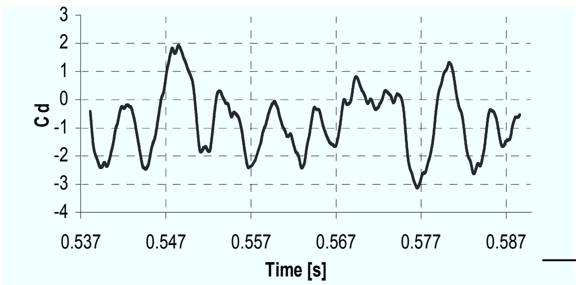

FFT

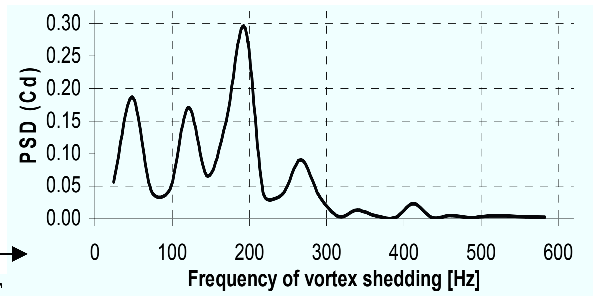

Fig.3. Drag coefficient Cd in the y direction (normal to the axis, see fig.2).

Fig.4. Spectral analysis of drag coefficient, frequency of vortex shedding (dominant f_v=194 Hz), PSD-Power Spectral Density.

From [9], the duration of the simulation can be determined beforehand by estimating the mean flow residence time *MFRT* in the solution domain. $MFRT = L/U$, where L is characteristic length of solution domain and U is characteristic mean flow velocity. The simulation should be run for at least a few mean flow residence times. In this case of lighting arrester the value of *MFRT* corresponds to the 0.014 s. The duration of the simulation was 3,6 *MFRT* corresponding to 0,05 s, which is recognizable in fig. 3 (drag coefficient indicates the force acting on the body). Then the frequency of vortex shedding f_v could be evaluated with the FFT to get the verification of accuracy of the solution. In fig. 4 the dominant frequency of vortex shedding is f_v=194 Hz.

Let's try to approximate the lightning arester by a much more simple body of a rotational cylinder. Experimental data are in [7]. It is known that Strouhal number for circumfluence of cylinder is constant (*Sh*=0.2) for large interval of Reynolds number *Re*=$3\cdot10^2-3.1\cdot10^5$. The Reynolds number *Re*=$2.5\cdot10^5$ for circumfluence of lightning arrester lies in this range. Then the Strouhal number could be resolved from $Sh=f_v\cdot D/U$. The value of diameter *D*=0.074 was estimated since *D* is variable along the lightning arrester's axes. The dominant Strouhal number for circumfluence of lightning arrester is 0.258.

In light of inner problem solution, after comparison of Strouhal number for both cases, it could be said, that the results are physically correct. The small difference could be induced due to different shape mainly different top of the lightning arrester or due to estimated diameter *D*.

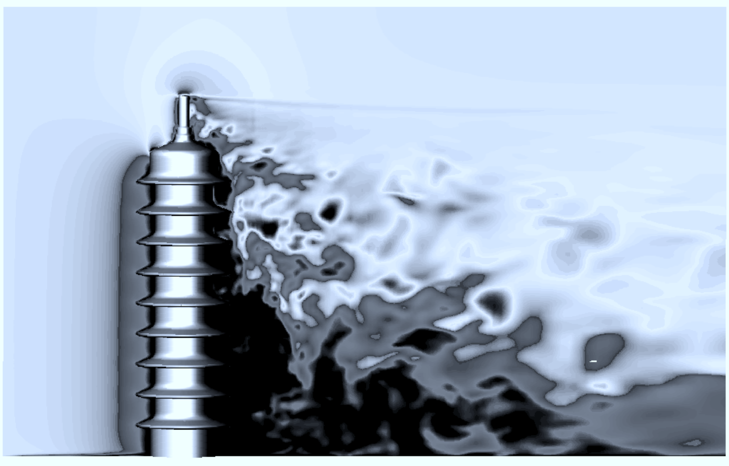

Fig. 5. Contours of velocity magnitude, M=0.19, *Re*=$2.5\cdot10^5$, Smagorinsky –Lilly subgrid scale model [8], $\Delta t=2.5\cdot10^{-5}$ *s*.

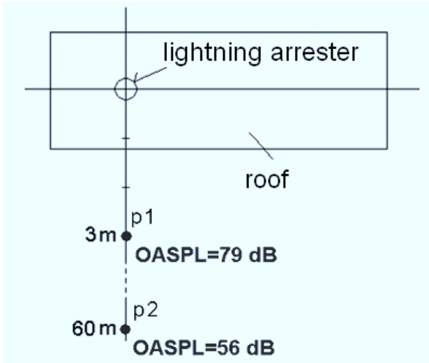

Fig. 6. Lightning arrester on the roof of electric locomotive – 4 *m* height (ground plan) and the locations of the receivers (p1, p2) – 1.7 *m* height.

3.3. Outer Problem Solution and the Results

After submitting the locations of the receivers P1 and P2 (fig. 6) to program Fluent the acoustic pressure is evaluated from the wave equation (11). The results are in form of time dependence of acoustic pressure, fig. 7, 8 (left), and frequency spectrum of sound pressure level SPL (right), which is acquired from FFT. The magnitude of sound pressure level is evaluated from $SPL(dB)=20\log_{10}(p_1/p_0)$, where p_1 is monitored acoustic pressure and p_0 is reference (the smallest audible) acoustic pressure of $2\cdot10^{-5}$ *Pa*. By integration over the frequency spectrum for given receiver, it is possible to evaluate the overall sound pressure level OASPL.

From fig. 7, 8, the acoustic pressure where observer location is 810D from lightning arrester's axes (receiver P2) is ten times smaller then in 40D (receiver P1). The magnitude of sound pressure level also increased from 79 dB to 56dB. The "noisy frequencies" are within 2000 Hz.

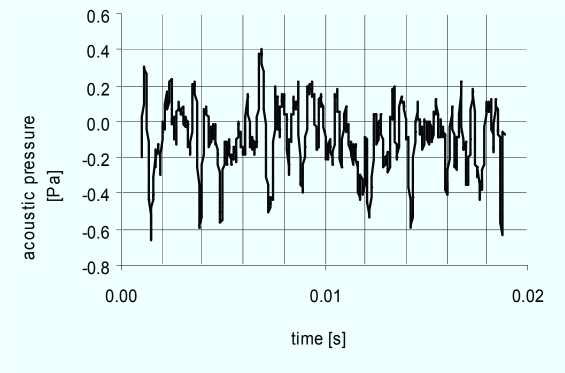

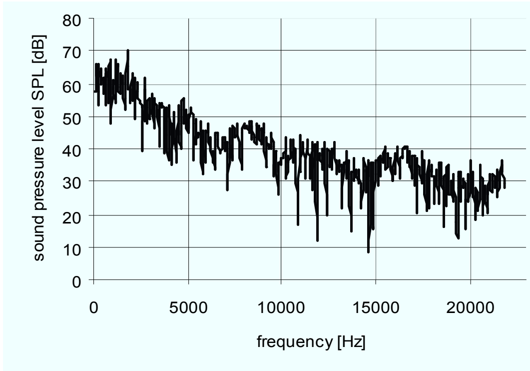

Fig.7. Acoustic pressure and frequency spectrum of sound pressure level, receiver p1 (fig. 6), observer location 40D (3 *m*) from lightning arrester's main axes, OASPL is 79 dB.

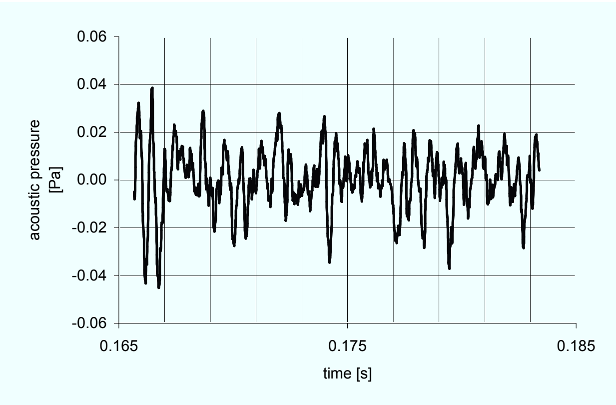

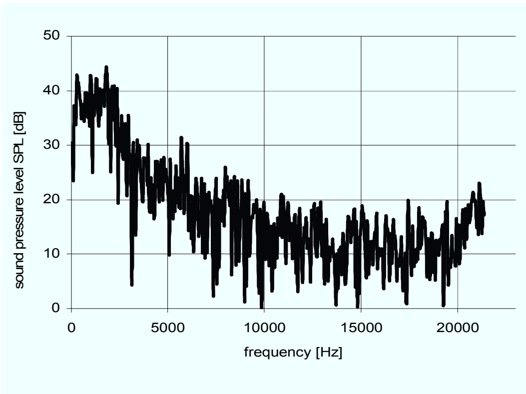

Fig.8. Acoustic pressure and frequency spectrum of sound pressure level, receiver p2 (fig. 6), observer location 810D (30 *m*) from lightning arrester's main axes, OASPL is 56 dB.

3.4. Broadband noise solution

This method is also based on Lighthill acoustic analogy [5], [6]. It is used for external aerodynamics for identification of the acoustic sources (position and intensity). The solutions of similar designs are compared to decrease the aerodynamically generated noise. In the case of lightning arrester, result represents acoustic power level on its surface. From fig. 9 the top of the lightning arrester is noisiest.

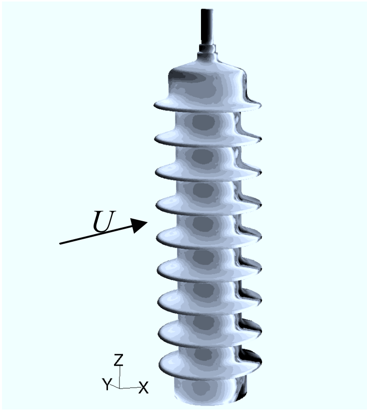

Fig.9. Contours of surface acoustic power level.

4. Conclusion

By Lighthill acoustic analogy as embodied in the FW-H equation the acoustic signal generated by lightning arrester in given receiver positions was acquired. Lightning arrester is positioned on the roof of an electric locomotive with the speed of 200 km/h. The solution was divided into two parts – inner problem solution, where the source data were acquired and outer problem solution, where the acoustic signal was evaluated in form of acoustic pressure and frequency spectrum of sound pressure level in given receiver positions.

Great effort has been given to the solution pre-processing, especially to get proper solution domain and proper fine mesh inside the source surface. The length of the smallest element has been set up with the respect to sinusoidal acoustic signal and the smallest wave length. Preliminary solution in form of the 2D cylinder example was numerically solved to get some estimation of the source surface shape for lightning arrester.

The accuracy of the solution was validated by comparison of Strouhal number for circumfluence of rotational cylinder and Strouhal number for circumfluence of lightning arrester (lightning arrester was approximate by a much more simple body of a rotational cylinder). The solution is physically correct, because the values of Strouhal number are very close. The small difference between them is caused by the shape difference (mainly - lightning arrester has different top). With the different acoustic approach (broadband) it was also found out, that this top of the lightning arrester is noisy.

Further work in progress will be significant in the improvement of the aeroacoustic solution consisting in modelling more source surfaces around the body. Then it will be possible to get some validation of the outer problem solution by comparison the results corresponding to each source surface, which corresponds to fine mesh creation.

The aeroacoustic data of lightning arrester must have been checked, because there have been doubts whether this lightning arrester positioned on the roof of electric locomotive in motion (speed of 200 km/h) is generating too much noise with its shape. Presented numerical solution showed that if the lightning arrester is the only aeroacoustic source on the roof, then OASPL of 79 dB in position p1 (fig. 6) would be acceptable. But such an ideal roof of electric locomotive does not really exist. There is also a noise generated by other mechanical sources. So it is necessary to perform another validation hereafter, where the acquired aeroacoustic data – aeroacoustic sources and also mechanical sources from whole locomotive, will be comprehended. To get some aeroacoustic data of a real roof of locomotive will be a problem of the future.

Acknowledgements

The work has been supported by the research project of SKODA TRANSPORTATION s.r.o. in connection with locomotive SKODA 109E production.

References

[1] K. S. Brentner, F. Farassat, An Analytical Comparison of the Acoustic Analogy and Kirchhoff Formulations for Moving Surfaces, AIAA Journal, 36(8), 1998.
[2] D. G. Crighton, A. P. Dowing, J. E. Ffowcs Williams, M. Heckl, F. G. Leppington, Modern Methods in Analytical Acoustic, Lecture Notes, Springer-Verlag, London, Chap. 11, Sec. 10. , 1992
[3] A. P. Dowing, J. E. Ffowcs Williams, Sound and Sources of Sound, Ellis Horwood, Chichester, England, UK, Chap. 9, Sec. 2. , 1983
[4] J. E. Ffowcs-Williams, D. L. Hawkings, Sound Generation by Turbulence and Surfaces in Arbitrary Motion, Proc. Royal Society of London, A264:321-342, 1969.
[5] M. J. Lighthill, On Sound Generated Aerodynamically I, Proceedings of the Royal Society of London, A211:564-587, 1952.
[6] M. J. Lighthill, On Sound Generated Aerodynamically. II, Turbulence as a Source of Sound, Proceedings of the Royal Society of London. Series A, Mathematical and Physical Sciences, Vol. 222, No. 1148 (Feb. 23, 1954), pp. 1-32.
[7] J. Linhart, Elasticity in Aerodynamics, ZCU in Pilsen, 2001.
[8] J. Smagorinsky, General Circulation Experiments with the Primitive Equations. I, The Basic Experiment, Month. Wea. Rev., 91:99-164, 1963
[9] Fluent 6.3 Documentation, User's Guide, 21. Predicting Aerodynamically Generated Noise, 12. Modeling Turbulence, Fluent Inc. 2006.